Characterization of Paper-Like Material Prepared from Chitosan/Graphene Oxide Composite

Thi Sinh Vo[1]* iD **, Tran Thi Bich Chau Vo[2]** iD

[1]Sungkyunkwan University, School of Mechanical Engineering, Suwon, 16419, Korea

[2]Can Tho University, Department of Industrial Management, Can Tho, Vietnam

Abstract: Chitosan (CTS) is considered to be a common biomacromolecule/poly-cationic compound containing the potential functional groups that can be utilized as a feedstock for novel materials. In this study, CTS/graphene oxide (CTS/GO, CG) mixtures were prepared at different conditions to confirm a suitable hydrogel formation, then applied to produce paper-like materials with various thickness via a simple casting method. As a result, the morphological structure finally yielded the paper-like materials (CG2 papers with varying numbers of casting times) with the layer-by-layer structures instead of the tightly-sticky paper-like structure (GO paper). Based on the possible interactions between the CTS molecules and GO nanosheets, the CG mixtures could also be determined by FTIR and Raman analysis; concomitantly, their thermal properties reach higher than that of the pure GO. Notably, the strong interactions and compatibility of the CTS molecules and GO nanosheets revealed good dispersion and interfacial adhesion, leading to significantly enhancing the mechanical properties of the CG2 paper-like materials with increasing number of casting times or compared to GO paper. Therefore, the CG2 paper-like materials with the various numbers of casting times fabricated in the present study can expose new approaches for the design and application of future foil/paper-like materials, as well as the desired thickness of these foil/paper-like materials can be controlled easily.

INTRODUCTION

Polymeric systems, as is well known, have been widely used in various research fields and practical applications (1-5). At same time, the most remarkable factors of a polymeric material were almost entirely physical, chemical, and interface properties. Thus, it is necessary to conduct considerable modification methods that can obtain better desired results corresponding to multiple research studies. Especially, foil/paper-like materials are concerned as integral parts of the current technological development owing to potential characteristic features (i.e.: protective layers, super-capacitors/electrical batteries, chemical /physical filters, molecular storage, adhesive layers, etc.) (5-10). Chitosan (CTS) is considered to be a typical biomacromolecule/poly-cationic compound with excellent properties (i.e.: low toxicity, antimicrobial activity, biocompatibility, appreciable biodegradability, admirable low immunogenicity, etc.) that has been utilized widely in various applications (i.e., biomedical, environmental, and food fields, etc.) (11). Basically, CTS is an extensively classified linear copolymer in natural material sources, especially in de-acetylation of chitin, which has become a potential candidate to be applied in lots of different research fields (3, 12-14).

Concomitantly, graphene oxide (GO) with potential functional groups has originated from a chemically modified graphene material, which can be incorporated with various organic macromolecules (15-17). Moreover, the GO material can be encouraged to fabricate the large-area paper-like materials for applications of thin-films/membranes with controlled permeability, super-capacitors, anisotropic ionic conductors, and molecular storage, etc. Besides, owing to the available hydrophilic nature of GO nanosheets, their paper-like structure can be used as a carrier substance to probably produce paper-like hybrid materials containing ceramics, polymers, or metals (11). More obviously, Singh et al. (18) reported a facile design and synthesis of magnetic iron oxide incorporated CTS/GO hydrogel nanocomposites by employing in situ mineralization of iron ions in a hydrogel matrix, which resulted in this material being able to enable dye removal in a wide variety of solution conditions and offering a promising platform for sustainable development of water purification technology. Whereas, Lyn et al. (19) investigated the application of active packaging from CTS incorporated with GO to maintain the quality and extend the storage life of palm-oil-based margarine. More notably, Menazea et al. (20) studied well the possible interactions between some divalent heavy metals and CTS/GO, which was based on the density functional theory (DFT) at B3LYP level with LANL2DZ basis set. Nonetheless, a foil/paper-like materials from GO-like structure is not commonly reported. In fact, the outstanding chemical and mechanical properties can yield a promising GO-based paper, as well as a paper-like material system that can be applied effectively in various practical applications.

In this study, the possible interaction mechanism of the CTS/GO (CG) mixtures without any cross-linker regarding CG hydrogel formation and damage was conducted on investigations of different parameters and conditions based on visual observations of different CG mixtures, and the mechanism involving thermo-induced hydrogel formation was explained in detail as well. Then, a suitable CG mixture was applied to produce paper-like materials with various thickness via a simple casting method. In particular, the chemical characterization, thermal properties and morphological structure of finally yielded paper-like materials were confirmed through several analysis instruments and compared with those of GO paper. Interestingly, the mechanical properties of the produced paper-like materials with increasing number of casting times were investigated as well, which revealed a dispersion and interfacial adhesion between CTS molecules and GO nanosheets inside the prepared CG mixtures. Hence, these paper-like materials with various numbers of casting times can expose new approaches for the design and desired thickness control of future foil/paper-like materials, as well as this paper-like material can be applied directly in various practical applications, i.e., heavy metals or organic dye removal, adsorption or filtration membranes, cell culture, super-capacitors, sensors, etc.

MATERIALS AND METHODS

Materials
Aqueous acetic acid solution and CTS powder (DD = ~85%) were obtained from Sigma–Aldrich. Aqueous GO dispersion was purchased from a Korean company.

Preparation of CG papers
CG mixtures at different conditions were prepared by blending CTS solution (1.00 g of CTS in 100 mL of 2.5% acetic acid solution) and aqueous GO dispersion (volume ratio of CTS/GO = 1/5, 1/10, and 1/15, v/v) (Table 1). The CG mixtures were stirred overnight for 2 – 3 days and sonicated for 10 min. The gelation/hydrogel formation of vials containing CG mixtures at room temperature (~80 °C) was confirmed via visual observation with a tube inversion. Next, the CG mixtures (~2.00 g) were cast on one substrate once, which was dried at room temperature. After that, an amount of CG mixtures (~2.00 g) was continued to be cast on the above CG paper and dried at room temperature, which was conducted until 2 – 5 times. The synthetic route of CG utilizing paper-like materials is shown in Fig. 1.
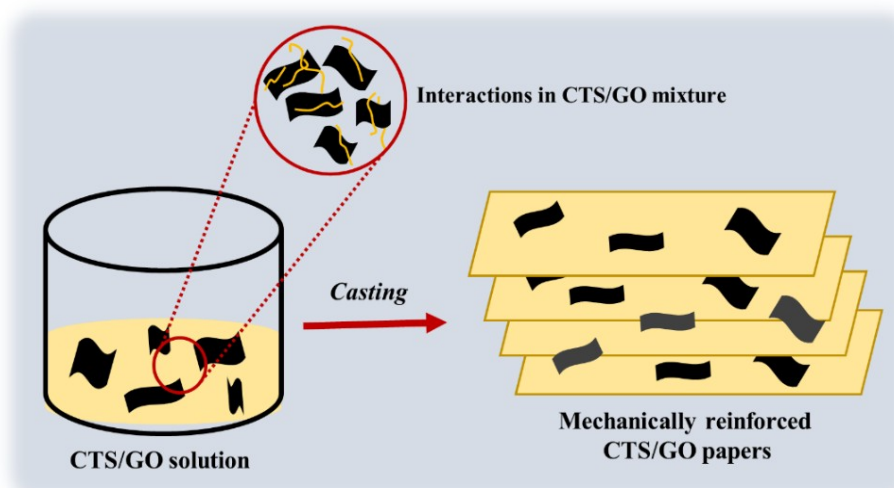
Figure 1: Synthetic route of CG utilizing as paper-like materials.

Table 1. Information of CGs.

Sample	CG1	CG2	CG3
Volume ratio of CTS/GO	1/5	1/10	1/15

Analysis instruments
SEM analysis
Morphological structures of the paper-like materials (top-surface and cross-section) were measured by a field-emission scanning electron microscope (FESEM) (JSM-7600F, JEOL) at different magnifications.

FT-IR and Raman analysis
The chemical characterization of the paper-like materials was analyzed by a Fourier-transform infrared (FT-IR) and Raman spectroscopies. FT-IR spectra was recorded on an Nicolet 380 system (Ietled Co.) using pellet – KBr method with a scanned 4000–400 cm^{-1} wavenumber. Raman spectra was scanned by an XperRam200 instrument with a laser wavelength of 405 nm.

Thermal gravimetric analysis
Thermal gravimetric analysis (TGA) was obtained on a Seiko Exstar6000 instrument with an applied 30–500 °C temperature range / 10 °C min^{-1} heating rate.

Tensile analysis
Typical stress–strain curves of the paper-like materials (1 cm x 5 cm original size) were measured by a universal tensile machine (UTM model 5565, UK) with 250 N of load cell at the pulling rate of 10 mm∢min^{-1}. Prior to the tensile test, the paper-like materials were stored for more than one day at room temperature. All reported results for the tensile tests were averages of three measured values.

RESULTS AND DISCUSSION

General observation
As known, CTS molecules and GO nanosheets contain several potential functional groups to be favorable in noncovalent interactions, which could operate a complex network formation between the CTS molecules and GO nanosheets to create a hydrogel state for a suitable CTS/GO (CG) mixture (11). In fact, these were also similarly presented in several previous lectures (21-24), especially in Zeta (ζ) potential of the CTS/GO composite (24). Basing on visual observation of the prepared CG mixtures under different conditions (Fig. 2), the CG2 mixture (volume ratio of CTS/GO = 1/10, Table 1) has formed a stable hydrogel state at both room temperature and ~80 °C (Fig. 2 B, E), as well as that hydrogel formation was still stable until be cooled to room temperature (Fig. 2H). The CG1 mixture (volume ratio of CTS/GO = 1/5, Table 1) was in a sol state at both room temperature (Fig. 2A) and ~80 °C (Fig. 2D) regarding deficient interactions between the CTS molecules and GO nanosheets, while the sol state of CG3 mixture (volume ratio of CTS/GO = 1/15, Table 1) only occurred at room temperature (Fig. 2C) and its gel state was at ~80 °C (Fig. 2F). Especially, a thermo-reversible gelation behavior has appeared in the CG3 mixture at ~80 °C (Fig. 2F), which could return to the sol state until cooled to room temperature

(Fig. 2I). Therefore, a damaged hydrogel state was negotiated through a gel−sol−gel transition, and the hydrogel formation could be renewed to its origin state in the CG3 mixture (11). As such, the CG2 mixture is seen as a CG mixture that has obtained optimal parameters and conditions to be applied to the next experiments.
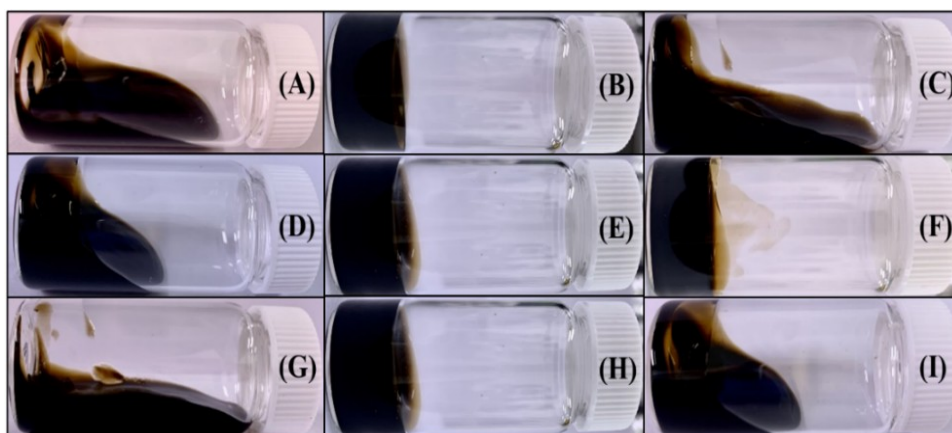

Figure 2: CTS/GO mixtures at room temperature [CG1 – (A), CG2 – (B), CG3 – (C)] and at ~80 °C [CG1 – (D), CG2 – (E), CG3 – (F)]. The CTS/GO mixtures [CG1 – (D), CG2 – (E), CG3 – (F)] are cooled to room temperature [CG1 – (G), CG2 – (H), CG3 – (I)].

To understand further the hydrogel state of various prepared CG mixtures, Fig. 3 shows the possible interaction mechanism of the CG mixtures at different conditions involving the CG hydrogel formation and damage. Basically, both CTS molecules and GO nanosheets contained lots of potential functional groups for the noncovalent interactions that have occurred in the CG hydrogel formation. Specifically, the noncovalent interactions could operate a complex network formation between the CTS molecules and GO nanosheets. Nonetheless, the mechanism regarding the thermo-induced hydrogel formation is still unclearl. Herein, the possible interactions in the CG mixtures could be encouraged with H_2O, CTS and GO (i.e.: $F_{H_2O–H_2O}$, $F_{CTS–CTS}$, $F_{GO–GO}$, $F_{H_2O–CTS}$, $F_{CTS–GO}$, $F_{H_2O–GO}$); concomitantly, the hydrogel formation has limited the interactions between CTS molecules and GO nanosheets with H_2O, especially at high temperatures. Specifically, the CG mixtures would contain electrostatic attraction interactions between the CTS molecules and GO nanosheets at room temperature, as well as the CTS chains being clustered because of a complexation in inter-/intra-molecular hydrogen bonds. As the weak hydrogen bonds among CTS chains increased, the interactions between the CTS chain and GO nanosheets became stronger with regard to the increase in their free motion at high temperature. As such, the stretched chains had lots of chances to interact with other GO nanosheets, as well as the entanglement possibility of CTS chains increased to form a complex network formation of them at the end. Herein, the CG2 mixture is chosen to be a representative mixture for the next analysis.
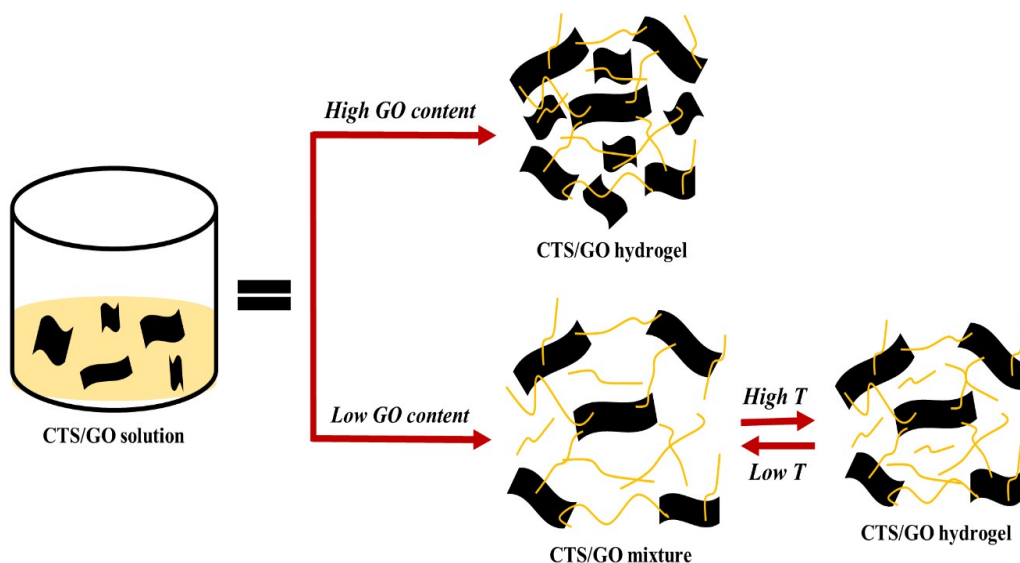
Figure 3: Possible interaction of CTS/GO mixtures at different conditions.

Chemical and thermal characterization of CTS/GO papers

-COO⁻ --- NH₃⁺: Electrostatic ion pairing
>C=O --- HN-: Hydrogen bonding
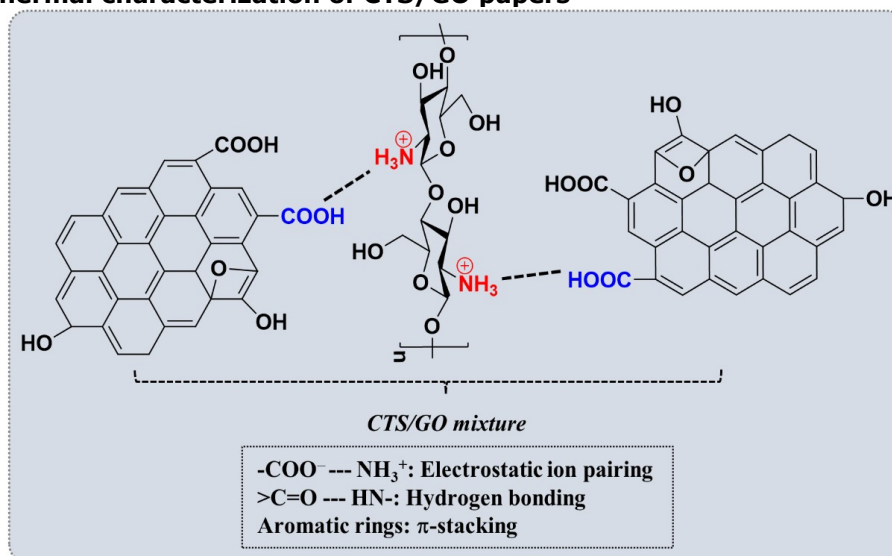Aromatic rings: π-stacking

Figure 4: Mechanism of chemical reaction between CTS and GO.

Fig. 4 shows that in the CTS/GO spectrum, the −COOH groups of GO interacted with the −NH$_3^+$ groups of CTS, resulting in strong hydrogen bonds and leading to a far more miscible CTS/GO mixture (11). The interfacial interactions among them can be very important to the corresponding properties of the CTS/GO, especially for a stable hybrid network structure (25, 26). More specifically, for chemical characterization of the prepared paper-like materials, FI-TR spectra were employed to investigate, as shown in Fig. 5 (A, B). In the pure CTS spectra (Fig. 5A), the characteristic peaks of symmetric/asymmetric −CH deformation, symmetric/asymmetric C−C−O stretching and C−C bending are observed at 1421.90 – 1383.03 cm^{-1}, 1081.92 – 1029.02 cm^{-1} and 663.42 – 516.85 cm^{-1}, respectively (5, 27, 28). Besides, the various peaks

have also appeared at 1159.87 cm^{-1} (C−O−C) and 897.04 cm^{-1} regarding the available saccharide structure of CTS (5, 28-30). In particular, the remaining characteristic peaks at 1652.32 – 1598.32 cm^{-1} have corresponded to −NH stretching/bending vibrations in −NH$_2$ groups (5, 27). While the pure GO spectra has revealed the peaks at 1734.25, 1632.36, 1400.01, 1229.96 and 1053.03 cm^{-1} corresponding to C=O carboxylic group, C=C alkenyl group, −OH deformation, C−O alkoxy group, and epoxy C−O−C stretching, respectively (31-33) (Fig. 5A). Especially, a broad peak was observed at 3700 – 3000 cm^{-1} regarding to −OH/−NH groups for all samples (Fig. 5B). In the CG2 paper's spectra, the peaks at 522.64 – 665.35 cm^{-1} and 1076.13 – 1019.96 cm^{-1} correspond to C−C bending and symmetric/asymmetric C−C−O

stretching vibrations, respectively. Interestingly, it also revealed that the characteristic peaks of saccharide structure of CTS and –OH deformation of GO have been moved to higher wavenumber regions such as at 1176.37 cm^{-1} (C–O–C), 899.70 cm^{-1} (C–O–C bridge) and 1412.05 cm^{-1} (–OH), indicating possible hydrogen bond formations between CTS and GO contained inside the CG mixtures. Furthermore, the peaks at 1753.05 cm^{-1} (C=O group) and 1669.76 – 1561.24 cm^{-1} (–NH/C=C groups) of CG2 paper were induced from the pure GO (C=O group, 1734.25 cm^{-1}) and CTS (–NH group, 1652.32 – 1598.32 cm^{-1}), respectively. However, these characteristic peaks have been not only moved to the higher wavenumber regions but also lower intensities compared with the pure materials, mainly due to the amide linkage formation (1669.76 cm^{-1}, –CONH$_2$) between carboxyl group (GO) and amino group (CTS), as reported in detail by Zhang et al. (25).

Concomitantly, two characteristic peaks of GO nanosheets were observed at 1348 cm^{-1} (D band) and 1605 cm^{-1} (G band) in both the pure GO and CG2 paper without a movement (Fig. 5C). Nonetheless, I$_D$/I$_G$ ratio of the CG2 paper (0.997) was higher than that of the pure GO (0.957) leading to a rising defect density of the CG2 paper. In other words, this increased defect could contribute significantly to the possible interactions in the CTS/GO mixtures. Moreover, thermal properties of the prepared paper-like materials were investigated by TGA instrument (Fig. 5D). The first loss weight occurred at ~50 °C regarding to the moisture loss for all samples, while the second loss weight of the CG2 paper was decomposed at 212.39 °C, as well as its thermal stability was better than that of pure GO (188.93 °C). Therefore, it was concluded that there were possible interactions (hydrogen bond, electrostatic attraction, and amide linkage formation) between the CTS molecules and GO nanosheets inside the CTS/GO mixtures (Fig. 3 and Fig. 4) through the above-analyzed FT-IR, Raman, and TGA results.
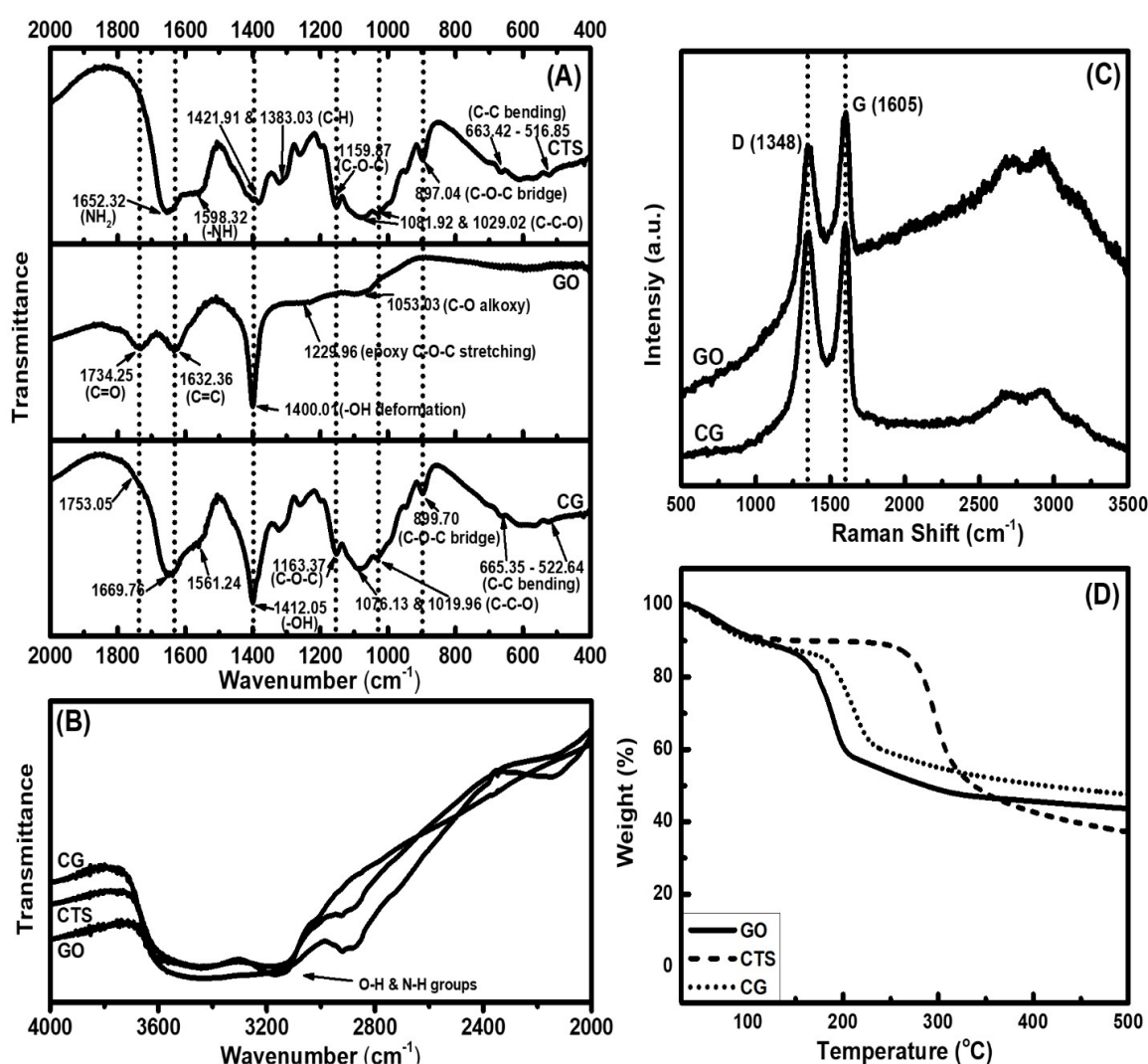

Figure 5: FTIR (A, B), Raman (C) and TGA curve of CTS, GO and CG2 paper.

Morphological properties of CTS/GO papers
For morphological properties of the prepared paper-like materials, SEM analysis was conducted (Fig. 6). The top-surface image of GO was considered to have a sheet-like structure (Fig. 6A), while its cross-sectional image was observed to be tightly-sticky paper-like structure owing to the available hydrophilic nature of GO nanosheets (Fig. 6B). For the prepared CG2 paper-like materials with the various numbers of casting times (Fig. 6 C – H), it was revealed that there was a strong network structure contained inside the CG2 mixture through the top-surface images of CG2 papers (Fig. 6 C – E). Specifically, the surface structure of CG2 papers (CG21 paper – CG2 paper with 1 casting time, CG23 paper – CG2 paper with 3 casting times, and CG25 paper – CG2 paper with 5 casting times) became wrinkled more instead of the sheet-like structure with the increasing number of casting times, probably due to the contraction of CTS chains in dry conditions. Concomitantly, the CTS particles were not observed in these top-surface images, suggesting that the CTS chains were well distributed inside the CG2 mixture as well as on the GO nanosheets. Moreover, the cross-sectional images of CG2 papers (Fig. 6 F – H) showed that the amount of CG2 mixture was supplemented further with the increasing number of casting times, leading to being deposited and stackedly-arranged like a layer-by-layer structure instead of the tightly-sticky paper-like structure, mainly due to the polymer backbone length of CTS on the GO nanosheets. Thereby, the strong electrostatic interactions between carboxyl group (GO) and amino group (CTS), as well as amide linkage formation ($-CONH_2$) have effectively occurred in the CG2 mixture (Fig. 3 and Fig. 4). Overall, the simple casting method could be considered as one of efficient methods to fabricate various foil/paper-like materials, as the desired thickness of foil/paper-like materials can also be controlled easily. Herein, the final thickness of paper-like materials reached about 4.750±0.132 µm; 5.125±0.441 µm; 6.625±0.205 µm and 11.625±0.383 µm for the GO, CG21, CG23, and CG25 papers, respectively.
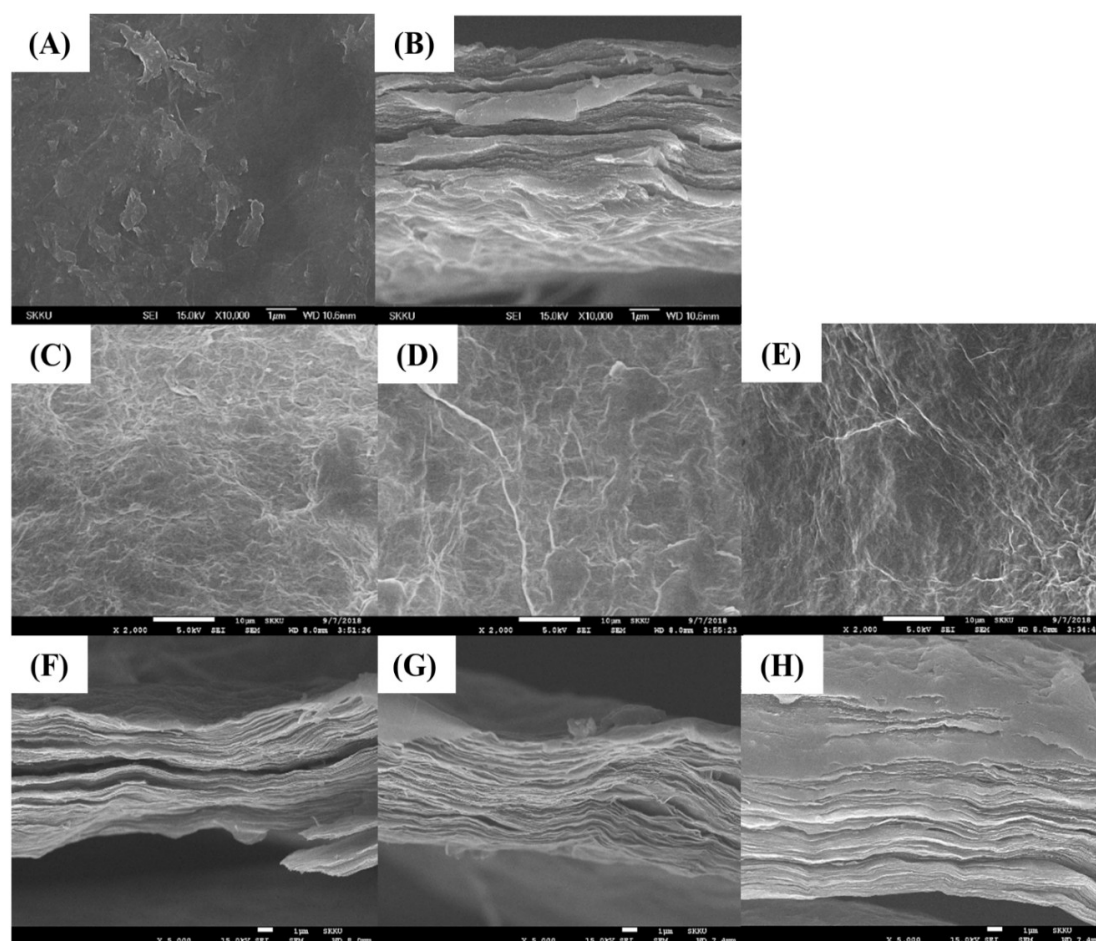

Figure 6: SEM images of GO [top-surface – (A) and cross-section – (B)]; various CG2 papers [top-surface: (C – E), and cross-section – (F – H)]: CG21 (C, E), CG23 (D, G) and CG25 (E, H).

Mechanical properties of CTS/GO papers

In addition to the above-mentioned characterization and morphological properties, the mechanical properties are also considered to be one of the important features for the paper-like materials (GO, CG2 papers with various numbers of casting times) based on the tensile tests at room temperature. Typical stress–strain curves for GO paper and CG2 papers with various numbers of casting times are shown in Fig. 7 [Digital camera images of CG2 paper − (A) and from tensile loading − (B)]. For the GO paper, its tensile strength, elongation at break, and modulus ($\varepsilon = \sim 0.5\%$) were lower than those of CG papers (GO paper: δ= 5.19 MPa, ε = 2.36%, and E = 1.83 MPa) relating to the hydrogen bond and van der Waals forces within the GO nanosheets of the produced GO paper (34). While the tensile strength and modulus ($\varepsilon = \sim 0.5\%$) of CG papers increased significantly with increasing number of casting times (19.21 MPa & 1.95 MPa / CG21 paper, 22.77 MPa & 2.55 MPa / CG23 paper, and 26.81 MPa & 2.64 MPa / CG25 paper), there

was only a small decrease in the elongation at break of CG23 paper (5.46% / CG21 paper, 4.94% / CG23 paper, and 5.74% / CG25 paper). Thereby, the enhancement of tensile strength and modulus of the CG papers manifests good dispersion of both CTS molecule and GO nanosheets, as well as their strong interactions (hydrogen bond, electrostatic attraction, and amide linkage formation) inside the CTS/GO mixtures. Concomitantly, the increase in tensile strength and modulus of CG papers exhibited stiffer behavior, implying a transition in their intermolecular interactions with increasing CG2 loading. In other words, the resultant hydrogen bond, electrostatic attraction, and amide linkage formation between the CTS molecules and GO nanosheets have supported rearrangements in the CG2 paper-like structures (layer-by-layer structure), leading to increased steric hindrance and lowering the torsion of the polymer backbone, as well as strong interlayer interactions in the CG2 papers (35-38).
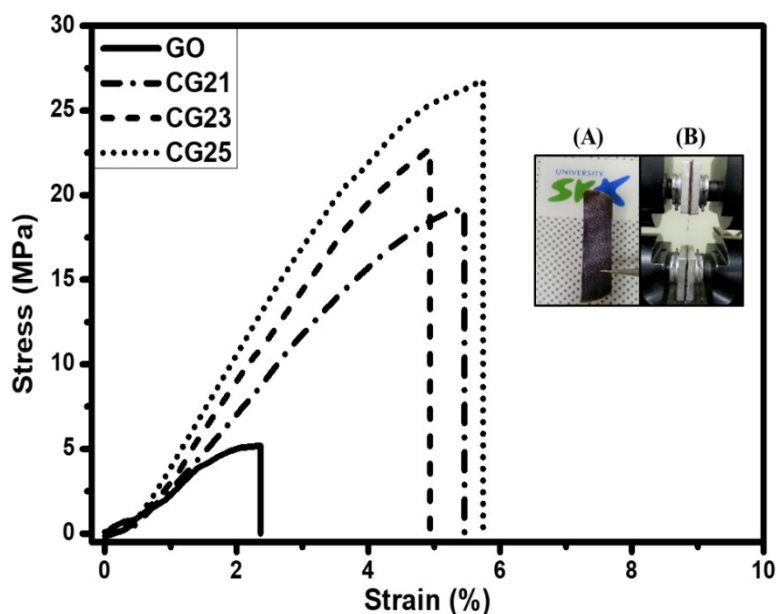

Figure 7: Typical stress–strain curves of the paper-like materials (GO, CG2 papers with various number of casting times). Digital camera images of CG2 paper (A) and paper from tensile loading (B).

Overall, good dispersion and interfacial stress transfer are considered significant factors in preparing the mechanically reinforced paper-like materials. It causes a more uniform stress distribution as well as minimizes the presence of the stress concentration center (39). As mentioned above, the GO nanosheets with oxygen-containing groups and negative charges can interact well with the CTS molecules – poly-cationic compounds through hydrogen bond, electrostatic attraction and amide linkage formation (Fig. 3 and Fig. 4). Furthermore, the contraction and backbone length of the CTS chains on the GO nanosheets promote stress transfer under dry conditions. Additionally,

the strong interactions and compatibility between the CTS molecules and GO nanosheets significantly increase the unidirectional dispersion of GO nanosheets in the CTS molecules as well as the interfacial adhesion, leading to significantly enhanced mechanical properties of the CG2 paper-like materials.

CONCLUSIONS

A simple casting method has yielded the paper-like materials (CG2 papers the various casting times) possessing layer-by layer structures instead of the tightly-sticky paper-like structures (GO paper)

based on the morphological properties (top-surface and cross-sectional SEM images). Besides, the strong interactions (hydrogen bond, electrostatic attraction, and amide linkage formation) between the CTS molecules and GO nanosheets have been determined through the FTIR and Raman results, as well as the thermal property has also become more stable in the prepared mixture with the CTS molecules and GO nanosheets. Moreover, the strong interactions and compatibility of them indicated good dispersion and interfacial adhesion, leading to significantly enhancing the mechanical properties of the CG2 paper-like materials with an increasing number of casting times or compared to GO paper. Therefore, the CG2 paper-like materials with the various numbers of casting times prepared in the present study can open up new avenues for the design and application of future foil/paper-like materials, as well as the desired thickness of these foil/paper-like materials can be controlled easily.

REFERENCES

1. Vo TS, Vo TTBC. Preparation and Characterization of Bis-Propargyl-Succinate, and its Application in Preliminary Healing Ability of Crosslinked Polyurethane using" Azide-Alkyne" Click. Journal of Engineering Science & Technology Review. 2020;13(4).

2. Vo TS, Vo TTBC, TiEn TT, SiNh NT. Enhancement of mechanical property of modified polyurethane with bis-butyl succinate. JOTCSA. 2021 Mar 30;8(2):519–26. <DOI>.

3. Vo TS, Vo TTBC. A Self-Healing Material Based on Microcapsules of Poly(Urea-Formaldehyde)/Bis-Propargyl-Succinate Containing in Polyurethane Matrix. JOTCSA. 2021 Jul 26;8(3):787–802. <DOI>.

4. Vo TS, Vo TTTN, Chau TTB. Preparation and Characterization of Microcapsules Containing Canola Oil with Poly (urea-formaldehyde) Shell and its Stability. Journal of Engineering Science & Technology Review. 2021;14(4):21–36.

5. Vo TS, Vo TTBC, Nguyen TS, TiEn TT. Fabrication and Characterization of Gelatin/Chitosan Hydrogel Utilizing as Membranes. Journal of the Turkish Chemical Society Section A: Chemistry. 2021 Oct 1;8(4): 1045–56. <DOI>.

6. Pitkethly MJ. Nanomaterials – the driving force. Materials Today. 2004 Dec;7(12):20–9. <DOI>.

7. Reynolds R, Greinke R. Influence of expansion volume of intercalated graphite on tensile properties of flexible graphite. Carbon. 2001;3(39):479–81.

8. Hennrich F, Lebedkin S, Malik S, Tracy J, Barczewski M, Rösner H, et al. Preparation, characterization and applications of free-standing single walled carbon nanotube thin films. Phys Chem Chem Phys. 2002 May 20;4(11):2273–7. <DOI>.

9. Coleman JN, Blau WJ, Dalton AB, Muñoz E, Collins S, Kim BG, et al. Improving the mechanical properties of single-walled carbon nanotube sheets by intercalation of polymeric adhesives. Appl Phys Lett. 2003 Mar 17;82(11):1682–4. <DOI>.

10. Berhan L, Yi YB, Sastry AM, Munoz E, Selvidge M, Baughman R. Mechanical properties of nanotube sheets: Alterations in joint morphology and achievable moduli in manufacturable materials. Journal of Applied Physics. 2004 Apr 15;95(8):4335–45. <DOI>.

11. Vo TS. Progresses and expansions of chitosan-graphene oxide hybrid networks utilizing as adsorbents and their organic dye removal performances: A short review. Journal of the Turkish Chemical Society Section A: Chemistry. 2021 Oct 18;8(4):1121–36. <DOI>.

12. Velmurugan N, Kumar GG, Han SS, Nahm KS, Lee YS. Synthesis and characterization of potential fungicidal silver nano-sized particles and chitosan membrane containing silver particles. Iranian Polymer Journal. 2009;18(5(107)):383–92.

13. Jiao TF, Zhou J, Zhou J, Gao L, Xing Y, Li X. Synthesis and characterization of chitosan-based Schiff base compounds with aromatic substituent groups. Iranian Polymer Journal. 2011;20(2):123–36.

14. Rao KK, Rao KM, Kumar PN, Chung ID. Novel chitosan-based pH sensitive micro-networks for the controlled release of 5-fluorouracil. Iranian Polymer Journal. 2010;19(4):265–76.

15. Xu Y, Wu Q, Sun Y, Bai H, Shi G. Three-Dimensional Self-Assembly of Graphene Oxide and DNA into Multifunctional Hydrogels. ACS Nano. 2010 Dec 28;4(12):7358–62. <DOI>.

16. Tung VC, Kim J, Cote LJ, Huang J. Sticky Interconnect for Solution-Processed Tandem Solar Cells. J Am Chem Soc. 2011 Jun 22;133(24):9262–5. <DOI>.

17. Bai H, Li C, Wang X, Shi G. On the Gelation of Graphene Oxide. J Phys Chem C. 2011 Apr 7;115(13):5545–51. <DOI>.

18. Singh N, Riyajuddin S, Ghosh K, Mehta SK, Dan A. Chitosan-Graphene Oxide Hydrogels with Embedded Magnetic Iron Oxide Nanoparticles for Dye Removal. ACS Appl Nano Mater. 2019 Nov 22;2(11):7379–92. <DOI>.

19. Han Lyn F, Tan CP, Zawawi RM, Nur Hanani ZA. Physicochemical properties of chitosan/ graphene oxide composite films and their effects on storage stability of palm-oil based margarine. Food Hydrocolloids. 2021 Aug;117:106707. <DOI>.

20. Menazea AA, Ezzat HA, Omara W, Basyouni OH, Ibrahim SA, Mohamed AA, et al. Chitosan/graphene oxide composite as an effective removal of Ni, Cu, As, Cd and Pb from wastewater. Computational and Theoretical Chemistry. 2020 Nov;1189:112980. <DOI>.

21. Januário EFD, Vidovix TB, Beluci N de CL, Paixão RM, Silva LHBR da, Homem NC, et al. Advanced graphene oxide-based membranes as a potential alternative for dyes removal: A review. Science of The Total Environment. 2021 Oct;789:147957. <DOI>.

22. Sharma P, Das MR. Removal of a Cationic Dye from Aqueous Solution Using Graphene Oxide Nanosheets:

Investigation of Adsorption Parameters. J Chem Eng Data. 2013 Jan 10;58(1):151–8. <DOI>.

23. Kahya N, Erim FB. Graphene oxide/chitosan-based composite materials as adsorbents in dye removal. Chemical Engineering Communications. 2021 Oct 6;1–16. <DOI>.

24. Sabzevari M, Cree DE, Wilson LD. Graphene Oxide–Chitosan Composite Material for Treatment of a Model Dye Effluent. ACS Omega. 2018 Oct 31;3(10):13045–54. <DOI>.

25. Zhang H ping, Yang B, Wang ZM, Xie C, Tang P, Bian L, et al. Porous graphene oxide/chitosan nanocomposites based on interfacial chemical interactions. European Polymer Journal. 2019 Oct;119:114–9. <DOI>.

26. Yang X, Tu Y, Li L, Shang S, Tao X ming. Well-Dispersed Chitosan/Graphene Oxide Nanocomposites. ACS Appl Mater Interfaces. 2010 Jun 23;2(6):1707–13. <DOI>.

27. Mansur HS, Mansur AAP, Curti E, De Almeida MV. Functionalized-chitosan/quantum dot nano-hybrids for nanomedicine applications: towards biolabeling and biosorbing phosphate metabolites. J Mater Chem B. 2013;1(12):1696. <DOI>.

28. El Ichi S, Zebda A, Alcaraz JP, Laaroussi A, Boucher F, Boutonnat J, et al. Bioelectrodes modified with chitosan for long-term energy supply from the body. Energy Environ Sci. 2015;8(3):1017–26. <DOI>.

29. Vo TS, Vo TTBC, Nguyen TS, Pham ND. Incorporation of hydroxyapatite in crosslinked gelatin/chitosan/poly(vinyl alcohol) hybrids utilizing as reinforced composite sponges, and their water absorption ability. Progress in Natural Science: Materials International. 2021 Oct;31(5):664–71. <DOI>.

30. Vo TS, Vo TTBC, Tran TT, Pham ND. Enhancement of water absorption capacity and compressibility of hydrogel sponges prepared from gelatin/chitosan matrix with different polyols. Progress in Natural Science: Materials International. 2022 Feb;32(1):54–62. <DOI>.

31. Bano S, Mahmood A, Kim SJ, Lee KH. Graphene oxide modified polyamide nanofiltration membrane with improved flux and antifouling properties. J Mater Chem A. 2015;3(5):2065–71. <DOI>.

32. Shen L, Xiong S, Wang Y. Graphene oxide incorporated thin-film composite membranes for forward osmosis applications. Chemical Engineering Science. 2016 Apr;143:194–205. <DOI>.

33. He D, Peng Z, Gong W, Luo Y, Zhao P, Kong L. Mechanism of a green graphene oxide reduction with reusable potassium carbonate. RSC Adv. 2015;5(16):11966–72. <DOI>.

34. Dikin DA, Stankovich S, Zimney EJ, Piner RD, Dommett GHB, Evmenenko G, et al. Preparation and characterization of graphene oxide paper. Nature. 2007 Jul;448(7152):457–60. <DOI>.

35. Wool RP, Statton WO. Dynamic polarized infrared studies of stress relaxation and creep in polypropylene. J Polym Sci Polym Phys Ed. 1974 Aug;12(8):1575–86. <DOI>.

36. Wool RP. Mechanisms of frequency shifting in the infrared spectrum of stressed polymer. J Polym Sci Polym Phys Ed. 1975 Sep;13(9):1795–808. <DOI>.

37. Wool RP. Infrared studies of deformation in semicrystalline polymers. Polym Eng Sci. 1980 Aug;20(12):805–15. <DOI>.

38. Ward IM, Hadley DW. An introduction to the mechanical properties of solid polymers. 1993. ISBN: 0-471-93874-2.

39. Coleman JN, Khan U, Gun'ko YK. Mechanical Reinforcement of Polymers Using Carbon Nanotubes. Adv Mater. 2006 Mar 17;18(6):689–706. <DOI>.